

Accepted Manuscript

Synthesis, characterization and crystal structures of vanadium(V) complexes derived from halido-substituted tridentate hydrazone compounds with antimicrobial activity

Ling-Yan He, Xiao-Yang Qiu, Jun-Yan Cheng, Shu-Juan Liu, Su-Min Wu

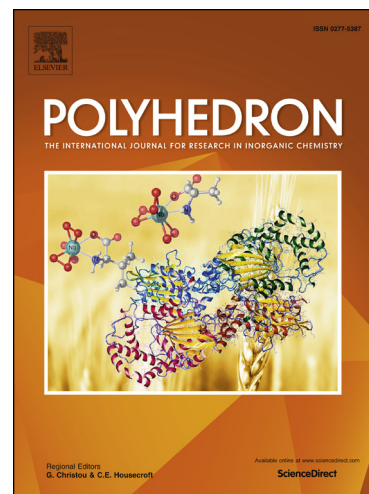
PII: S0277-5387(18)30569-2
DOI: <https://doi.org/10.1016/j.poly.2018.09.017>
Reference: POLY 13416

To appear in: *Polyhedron*

Received Date: 11 May 2018
Revised Date: 6 September 2018
Accepted Date: 7 September 2018

Please cite this article as: L-Y. He, X-Y. Qiu, J-Y. Cheng, S-J. Liu, S-M. Wu, Synthesis, characterization and crystal structures of vanadium(V) complexes derived from halido-substituted tridentate hydrazone compounds with antimicrobial activity, *Polyhedron* (2018), doi: <https://doi.org/10.1016/j.poly.2018.09.017>

This is a PDF file of an unedited manuscript that has been accepted for publication. As a service to our customers we are providing this early version of the manuscript. The manuscript will undergo copyediting, typesetting, and review of the resulting proof before it is published in its final form. Please note that during the production process errors may be discovered which could affect the content, and all legal disclaimers that apply to the journal pertain.



Synthesis, characterization and crystal structures of vanadium(V) complexes derived from halido-substituted tridentate hydrazone compounds with antimicrobial activity

Ling-Yan He^a, Xiao-Yang Qiu^{a,*}, Jun-Yan Cheng^b, Shu-Juan Liu^a, Su-Min Wu^a

^a *College of Science & Technology, Ningbo University, Ningbo 315212, P.R. China*

^b *College of Chemistry, Chemical Engineering and Material Science, Shandong Normal University, Jinan 250014, P.R. China*

* *e-mail: xiaoyang_qiu@126.com*

Abstract

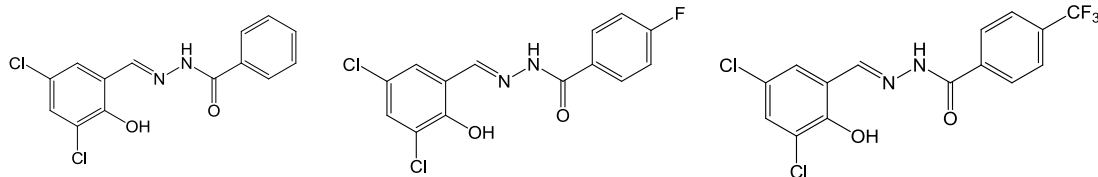
Three new chlorido-substituted hydrazone compounds *N'*-(3,5-dichloro-2-hydroxybenzylidene)benzohydrazide (H_2L^1), *N'*-(3,5-dichloro-2-hydroxybenzylidene)-4-fluorobenzohydrazide (H_2L^2) and *N'*-(2-hydroxy-3-methylbenzylidene)-4-trifluoromethylbenzohydrazide (H_2L^3), were prepared and characterized by IR, UV-Vis and ¹H NMR spectra. Based on the hydrazone compounds, three new vanadium(V) complexes, $[VOL^1(OEt)(EtOH)] \cdot [VOL^1(OEt)(MeOH)]$ (**1**), $[VOL^2(OEt)(EtOH)]$ (**2**) and $[VOL^3(OEt)(EtOH)]$ (**3**), were prepared and characterized by IR and UV-Vis spectra, as well as single crystal X-ray diffraction. X-ray analysis indicates that the complexes are mononuclear vanadium(V) species, with the V atoms coordinated in octahedral geometry. The hydrazone compounds and their vanadium complexes were evaluated against the bacteria *Bacillus subtilis*, *Staphylococcus aureus*, *Escherichia coli*, and *Pseudomonas fluorescense*, and the fungi *Candida albicans* and *Aspergillus niger*. The existence of the fluoro groups in the hydrazone ligands can improve the

antibacterial activities.

Keywords: Hydrazone; Vanadium complex; Mononuclear complex; Crystal structure; Antimicrobial activity

1. Introduction

Hydrazones with the typical functional group $-\text{CH}=\text{N}-\text{NH}-\text{C}(\text{O})-$ are a kind of biological active compound. The compounds have attracted remarkable attention for their wide range of biological activities, such as antibacterial [1-3], antifungal [4,5], and antitumor [6,7]. It was reported that compounds bearing electron-withdrawing groups can improve their antimicrobial activities [8,9]. Rai and co-workers reported a series of fluoro, chloro, bromo, and iodo-substituted compounds, and found that they have significant antimicrobial activities [10]. Vanadium complexes with Schiff bases and hydrazones have been reported to have interesting antibacterial activities [11-14]. As a continuation of work on the exploration of novel complex based antimicrobial agents, in this paper, chloro and fluoro groups are incorporated in hydrazone compounds, and then coordinate with vanadium, to form three new halido-substituted hydrazone compounds $N'-(3,5\text{-dichloro-2-hydroxybenzylidene})\text{benzohydrazide}$ (H_2L^1), $N'-(3,5\text{-dichloro-2-hydroxybenzylidene})\text{-4-fluorobenzohydrazide}$ (H_2L^2) and $N'-(2\text{-hydroxy-3-methylbenzylidene})\text{-4-trifluoromethylbenzohydrazide}$ (H_2L^3), and three new vanadium(V) complexes, $[\text{VOL}^1(\text{OEt})(\text{EtOH})]$ (**1**), $[\text{VOL}^2(\text{OEt})(\text{EtOH})]$ (**2**) and $[\text{VOL}^3(\text{OEt})(\text{EtOH})]$ (**3**), and studied their antimicrobial activities.



H_2L^1 H_2L^2 H_2L^3

2. Experimental

2.1. Materials and methods

3,5-Dichlorosalicylaldehyde, benzohydrazide, 4-fluorobenzohydrazide, 4-trifluoromethylbenzohydrazide, and VO(acac)₂ were purchased from Sigma-Aldrich and used as received. All other reagents were of analytical reagent grade. Elemental analyses of C, H and N were carried out in a Perkin-Elmer automated model 2400 Series II CHNS/O analyzer. FT-IR spectra were obtained on a Perkin-Elmer 377 FT-IR spectrometer with samples prepared as KBr pellets. UV-Vis spectra were obtained on a Lambda 35 spectrometer. ¹H NMR data were recorded on Bruker 300 MHz spectrometer. X-ray diffraction was carried out on a Bruker APEX II CCD diffractometer.

2.2. Synthesis of the hydrazones

To the ethanolic solution (30 mL) of 3,5-dichlorosalicylaldehyde (0.01 mol, 1.91 g) was added an ethanolic solution (20 mL) of benzohydrazide (0.01 mol, 1.36 g), 4-fluorobenzohydrazide (0.01 mol, 1.54 g) or 4-trifluoromethylbenzohydrazide (0.01 mol, 2.04 g) with stirring. The mixtures were stirred for 30 min at room temperature, and left to slowly evaporate to give colorless crystalline product, which were recrystallized from ethanol and dried in vacuum containing anhydrous CaCl₂.

For H_2L^1 : Yield 92%. IR data (cm⁻¹): 3454, 3190, 1643, 1596. UV-Vis data (MeOH, λ_{max} , nm): 290, 303, 332, 400. *Anal.* Calc. for C₁₄H₁₀Cl₂N₂O₂: C, 54.4; H, 3.3; N, 9.1. Found: C, 54.6; H, 3.2; N, 9.0%. ¹H NMR (300 MHz, *d*⁶-DMSO): δ 12.52 (s, 1H, OH), 11.18 (s, 1H, NH), 8.58 (s, 1H, CH=N), 7.97 (d, 2H, ArH), 7.63 (m, 1H, ArH), 7.57 (d, 2H, ArH), 7.37 (m, 2H, ArH). For H_2L^2 : Yield 95%. IR data (cm⁻¹):

3451, 3212, 1648, 1597. UV-Vis data (MeOH, λ_{\max} , nm): 240, 290, 330, 400. *Anal.* Calc. for $C_{14}H_9Cl_2FN_2O_2$: C, 51.4; H, 2.8; N, 8.6. Found: C, 51.3; H, 2.8; N, 8.5%. 1H NMR (300 MHz, d^6 -DMSO): δ 12.50 (s, 1H, OH), 11.26 (s, 1H, NH), 8.57 (s, 1H, CH=N), 8.03 (d, 2H, ArH), 7.65 (d, 2H, ArH), 7.37 (m, 2H, ArH). For H_2L^3 : Yield 93%. IR data (cm^{-1}): 3445, 3182, 1645, 1598. UV-Vis data (MeOH, λ_{\max} , nm): 290, 301, 332, 400. *Anal.* Calc. for $C_{15}H_9Cl_2F_3N_2O_2$: C, 47.8; H, 2.4; N, 7.4. Found: C, 47.6; H, 2.5; N, 7.5%. 1H NMR (300 MHz, d^6 -DMSO): δ 12.46 (s, 1H, OH), 11.20 (s, 1H, NH), 8.57 (s, 1H, CH=N), 8.17 (d, 2H, ArH), 8.14 (d, 2H, ArH), 7.37 (m, 2H, ArH).

2.3. Synthesis of the complexes

The hydrazone compounds (0.1 mmol each) dissolved in ethanol were mixed with $VO(acac)_2$ (0.1 mmol, 26.5 mg) dissolved in methanol (10 mL). The mixtures were refluxed for 1 h and then cooled to room temperature. Single crystals of the complexes, suitable for X-ray diffraction, were grown from the solution upon slowly evaporation within a few days. The crystals were isolated by filtration, washed with ethanol and dried in vacuum containing anhydrous $CaCl_2$.

For **1**: Yield 51%. IR data (cm^{-1}): 3432 (w), 1607 (s), 972 (m). UV-Vis data (CH_3CN , λ_{\max} , nm): 255, 303, 405, 435. *Anal. calc.* for $C_{18}H_{18}Cl_2FN_2O_5V$: C, 44.7; H, 3.8; N, 5.8; found: C, 44.7; H, 3.7; N, 5.9%. For **2**: Yield 43%. IR data (cm^{-1}): 3437 (w), 1610 (s), 975 (m). UV-Vis data (CH_3CN , λ_{\max} , nm): 262, 305, 410, 438. *Anal. calc.* for $C_{18}H_{18}Cl_2FN_2O_5V$: C, 44.7; H, 3.8; N, 5.8; found: C, 44.9; H, 3.6; N, 5.8%. For **3**: Yield 38%. IR data (cm^{-1}): 3421 (w), 1610 (s), 973 (m). UV-Vis data (CH_3CN , λ_{\max} , nm): 257, 300, 406, 435. *Anal. calc.* for $C_{19}H_{18}Cl_2F_3N_2O_5V$: C, 42.8; H, 3.4; N, 5.3; found: C, 42.9; H, 3.5; N, 5.1%.

2.4. X-ray crystallography

X-ray diffraction was carried out at a Bruker APEX II CCD area diffractometer equipped with MoK α radiation ($\lambda = 0.71073 \text{ \AA}$). The collected data were reduced with SAINT [15], and multi-scan absorption correction was performed using SADABS [16]. The structures of the complexes were solved by direct method, and refined against F^2 by full-matrix least-squares method using SHELXTL [17]. All of the non-hydrogen atoms were refined anisotropically. The hydrogen atoms of the methanol and ethanol ligands were located from electronic density maps and refined isotropically. The remaining hydrogen atoms were placed in calculated positions and constrained to ride on their parent atoms. The trifluoromethyl group of complex **3** was disordered over two sites, with occupancies of 0.514(3) and 0.486(3), respectively. The crystallographic data and refinement parameters for the complexes are listed in Table 1. Selected bond lengths and angles are listed in Table 2.

2.5. Antimicrobial assay

The antibacterial activities of the hydrazone compounds and the vanadium complexes were tested against *B. subtilis*, *S. aureus*, *E. coli*, and *P. fluorescens* using MH (Mueller–Hinton) medium. The antifungal activities of the compounds were tested against *C. albicans* and *A. niger* using RPMI-1640 medium. The MIC values of the tested compounds were determined by a colorimetric method using the dye MTT [18]. A stock solution of the compound ($150 \mu\text{g}\cdot\text{mL}^{-1}$) in DMSO was prepared and graded quantities ($75 \mu\text{g}\cdot\text{mL}^{-1}$, $37.5 \mu\text{g}\cdot\text{mL}^{-1}$, $18.8 \mu\text{g}\cdot\text{mL}^{-1}$, $9.4 \mu\text{g}\cdot\text{mL}^{-1}$, $4.7 \mu\text{g}\cdot\text{mL}^{-1}$, $2.3 \mu\text{g}\cdot\text{mL}^{-1}$, $1.2 \mu\text{g}\cdot\text{mL}^{-1}$, $0.59 \mu\text{g}\cdot\text{mL}^{-1}$) were incorporated in specified quantity of the corresponding sterilized liquid medium. A specified quantity of the medium containing the compound was poured into micro-titration plates. Suspension of the microorganism was prepared to contain approximately $1.0 \times 10^5 \text{ cfu}\cdot\text{mL}^{-1}$ and applied to microtitration plates with serially diluted compounds in DMSO to be tested and

incubated at 37 °C for 24 h and 48 h for bacteria and fungi, respectively. Then the MIC values were visually determined on each of the microtitration plates, 50 μL of PBS (phosphate buffered saline 0.01 $\text{mol}\cdot\text{L}^{-1}$, pH = 7.4) containing 2 mg of $\text{MTT}\cdot\text{mL}^{-1}$ was added to each well. Incubation was continued at room temperature for 4–5 h. The content of each well was removed and 100 μL of isopropanol containing 5% 1 $\text{mol}\cdot\text{L}^{-1}$ HCl was added to extract the dye. After 12 h of incubation at room temperature, the optical density was measured with a microplate reader at 550 nm.

3. Results and discussion

3.1. Synthesis and characterization

The hydrazone compounds H_2L^1 , H_2L^2 and H_2L^3 were readily prepared by the condensation reaction of a 1:1 molar ratio of 3,5-dichlorosalicylaldehyde with benzohydrazide, 4-fluorobenzohydrazide and 4-trifluoromethylbenzohydrazide, respectively in ethanol. The complexes were prepared by the reaction of the hydrazone compounds with vanadyl acetylacetonate in a mixture of methanol and ethanol, followed by recrystallization. Elemental analyses of the complexes are in accordance with the molecular structures proposed by the X-ray analysis.

3.2. Spectroscopic studies

In the spectra of the hydrazone compounds and the complexes, the weak and broad bands in the range 3300-3500 cm^{-1} are assigned to the vibration of O–H bonds. The weak and sharp bands of the hydrazone compounds located at about 3200 cm^{-1} are assigned to the vibration of N–H bonds. The intense bands at 1640-1650 cm^{-1} of the hydrazone compounds are generated by $\nu(\text{C}=\text{O})$ vibrations, whereas the bands at 1590-1600 cm^{-1} by the $\nu(\text{C}=\text{N})$ ones. The non-observation of the $\nu(\text{C}=\text{O})$ and $\nu(\text{N}-\text{H})$ bands, present in the spectra of the hydrazone compounds, indicates the enolization of

the amide functionality upon coordination to the V-center. Instead strong bands at 1607-1610 cm^{-1} are observed, which can be attributed to the asymmetric stretching vibration of the conjugated $\text{CH}=\text{N}-\text{N}=\text{C}-\text{O}$ groups, characteristic for the coordination of the enolate form of the compounds. The strong $\nu(\text{V}=\text{O})$ bands at 972-975 cm^{-1} for the complexes could be clearly identified for the complexes [19].

In the electronic spectra of the hydrazones and the complexes, the bands in the range of 300-340 nm are attributed to the intra-ligand $\pi \rightarrow \pi^*$ absorption. In the electronic spectra of the complexes, the lowest energy transition bands are observed at 420-450 nm, which are attributed to LMCT transition as charge transfer from *p*-orbital on the lone-pair of ligands' oxygen atoms to the empty *d*-orbital of the vanadium atoms. The other mainly LMCT and to some extent $\pi \rightarrow \pi^*$ bands appear at 250-270 nm for the complexes are due to the oxygen donor atoms bound to vanadium(V) [19].

3.3. Structure description of the complexes

Molecular structures of the complexes are shown in Figures 1-3, respectively. The asymmetric unit of complex **1** contains two vanadium complex molecules. One molecule contains a methanol and ethoxy ligands, and the other molecule contains an ethanol and ethoxy ligands. Complexes **2** and **3** contain ethanol and ethoxy ligands. In the complexes, the coordination geometry around the vanadium atoms can be described as distorted octahedral with the tridentate hydrazone ligand coordinated in meridional fashion, forming five- and six-membered chelate rings with bite angles of 73.7-74.0° and 83.9-84.3°, respectively, typical for this type of ligand systems [20]. Each chelating hydrazone ligand lies in a plane with one hydroxylato ligand which lies *trans* to the hydrazone imino N atom. One solvent O atom of the methanol or ethanol ligand *trans* to the oxo group completes the distorted octahedral coordination sphere at rather elongated distances of 2.3-2.4 Å, due to the *trans* influence of the oxo

group. This is accompanied by significant displacements of the vanadium atoms from the planes defined by the four basal donor atoms toward the apical oxo oxygen atoms by 0.28-0.32 Å. As expected, the hydrazone compounds coordinate in their doubly deprotonated enolate form which is consistent with the observed O2–C8 and N2–C8 bond lengths of about 1.30 Å. This agrees with reported vanadium complexes containing the enolate form of this ligand type [20-22].

In the crystal packing structure of complex **1**, the complex molecules are linked by methanol and ethanol ligands through intermolecular hydrogen bonds of O–H...N [O3–H3 = 0.85(1) Å, H3...N4ⁱ = 2.07(5) Å, O3...N4ⁱ = 2.88(1) Å, O3–H3...N4ⁱ = 158(12)°, symmetry code for i: $-1 + x, y, z$; O8–H8 = 0.85(1) Å, H8...N2 = 2.08(6) Å, O8...N2 = 2.87(1) Å, O8–H8...N2 = 154(11)°], leading to the formation of chains along the *a*-axis direction (Figure 4). In the crystal packing structure of complex **2**, the complex molecules are linked by ethanol ligands through intermolecular hydrogen bonds of O–H...N [O3–H3 = 0.93 Å, H3...N2ⁱⁱ = 1.95 Å, O3...N2ⁱⁱ = 2.869(4) Å, O3–H3...N2ⁱⁱ = 169(7)°, symmetry code for ii: $-x, 1 - y, -1 - z$], leading to the formation of chains along the *c*-axis direction (Figure 5). In the crystal packing structure of complex **3**, the complex molecules are linked by ethanol ligands through intermolecular hydrogen bonds of O–H...N [O3–H3 = 0.85(1) Å, H3...N2ⁱⁱⁱ = 2.08(3) Å, O3...N2ⁱⁱⁱ = 2.900(6) Å, O3–H3...N2ⁱⁱⁱ = 163(7)°, symmetry code for iii: $1 - x, 1 - y, 1 - z$], leading to the formation of chains along the *b*-axis direction (Figure 6).

3.4. Antimicrobial activity

The hydrazone compounds and the vanadium complexes were screened for antibacterial activities against two Gram (+) bacterial strains (*Bacillus subtilis* and *Staphylococcus aureus*) and two Gram (–) bacterial strains (*Escherichia coli* and *Pseudomonas fluorescense*) by MTT method. The MIC (minimum inhibitory

concentration, $\mu\text{g}\cdot\text{mL}^{-1}$) values of the compounds against four bacteria are listed in Table 3. Penicillin G was used as the standard drug. The hydrazone compound H_2L^1 shows weak activity against *B. subtilis* and *S. aureus*, and no activity against *P. fluorescence* and *E. coli*. The hydrazone compound H_2L^2 shows effective activity against *B. subtilis*, and medium activity against *S. aureus* and *E. coli*, and no activity against *P. fluorescence*. The hydrazone compound H_2L^3 shows effective activity against *B. subtilis* and *S. aureus*, and medium activity against *E. coli*, and no activity against *P. fluorescence*. The vanadium complexes, in general, have stronger activities against the bacteria than the free hydrazones. Moreover, complexes **2** and **3** have stronger activities than complex **1**. Complexes **2** and **3** have strong activities against *B. subtilis* and *S. aureus*, which are more effective than Penicillin G. However, the complexes have no activity against *P. fluorescence* and two fungal strains (*Candida albicans* and *Aspergillus niger*). From the results, we can conclude that the existence of the fluoro groups in the hydrazone ligands can improve the antibacterial activities.

Appendix A. Supplementary data

CCDC 1841526, 1841527 and 1841528 contains the supplementary crystallographic data for complexes **1**, **2** and **3**, respectively. These data can be obtained free of charge via <http://www.ccdc.cam.ac.uk/conts/retrieving.html>, or from the Cambridge Crystallographic Data Centre, 12 Union Road, Cambridge CB2 1EZ, UK; fax: (+44) 1223-336-033; or e-mail: deposit@ccdc.cam.ac.uk.

Acknowledgments

We thank the Educational Commission of Henan Province of China (Grant No. 14B150036) and the Natural Science Foundation of Henan Province of China (Grant

No. 142300410252) for supporting of this work.

References

- [1] Z.A. Kaplancikli, M.D. Altintop, A. Ozdemir, G. Turan-Zitouni, G. Goger, F. Demirci. *Lett. Drug Des. Discov.* 11 (2014) 355.
- [2] R. Narisetty, K.B. Chandrasekhar, S. Mohanty, B. Balram. *Lett. Drug Des. Discov.* 10 (2013) 620.
- [3] F. Zhi, N. Shao, Q. Wang, Y. Zhang, R. Wang, Y. Yang. *J. Struct. Chem.* 54 (2013) 148.
- [4] A. Ozdemir, G. Turan-Zitouni, Z.A. Kaplancikli, F. Demirci, G. Iscan. *J. Enzyme Inhib. Med. Chem.* 23 (2008) 470.
- [5] C. Loncle, J.M. Brunel, N. Vidal, M. Dherbomez, Y. Letourneux. *Eur. J. Med. Chem.* 39 (2004) 1067.
- [6] Y.-C. Liu, H.-L. Wang, S.-F. Tang, Z.-F. Chen, H. Liang. *Anticancer Res.* 34 (2014) 6034.
- [7] P. Krishnamoorthy, P. Sathyadevi, A.H. Cowley, R.R. Butorac, N. Dharmaraj. *Eur. J. Med. Chem.* 46 (2011) 3376.
- [8] M. Zhang, D.-M. Xian, H.-H. Li, J.-C. Zhang, Z.-L. You. *Aust. J. Chem.* 65 (2012) 343.
- [9] L. Shi, H.-M. Ge, S.-H. Tan, H.-Q. Li, Y.-C. Song, H.-L. Zhu, R.-X. Tan. *Eur. J. Med. Chem.* 42 (2007) 558.
- [10] N.P. Rai, V.K. Narayanaswamy, T. Govender, B.K. Manuprasad, S. Shashikanth, P.N. Arunachalam. *Eur. J. Med. Chem.* 45 (2010) 2677.
- [11] S.S. Wazalwar, N.S. Bhawe, A.G. Dikundwar, P. Ali. *Synth. React. Inorg. Met.-Org. Nano-Met. Chem.* 41 (2011) 459.

- [12]J.-L. Liu, M.-H. Sun, J.-J. Ma. Synth. React. Inorg. Met.-Org. Nano-Met. Chem. 45 (2015) 117.
- [13]Z.H. Chohan, S.H. Sumrra, M.H. Youssoufi, T.B. Hadda. Eur. J. Med. Chem. 45 (2010) 2739.
- [14]O. Taheri, M. Behzad, A. Ghaffari, M. Kubicki, G. Dutkiewicz, A. Bezaatpour, H. Nazari, A. Khaleghian, A. Mohammadi, M. Salehi. Transition Met. Chem. 39 (2014) 253.
- [15]Bruker, SMART (Version 5.625) and SAINT (Version 6.01). Bruker AXS Inc., Madison, Wisconsin, USA (2007).
- [16]G.M. Sheldrick. SADABS. Program for Empirical Absorption Correction of Area Detector, University of Göttingen, Germany (1996).
- [17]G.M. Sheldrick. SHELXTL V5.1 Software Reference Manual, Bruker AXS, Inc., Madison, Wisconsin, USA (1997).
- [18]J. Meletiadis, J.F.G.M. Meis, J.W. Mouton, J.P. Donnelly, P.E. Verweij. J. Clin. Microbiol. 38 (2000) 2949.
- [19]A. Sarkar, S. Pal. Polyhedron 26 (2007) 1205.
- [20]H.H. Monfared, S. Alavi, R. Bikas, M. Vahedpour, P. Mayer. Polyhedron 29 (2010) 3355.
- [21]X.-T. Zhang, X.-P. Zhan, D.-M. Wu, Q.-Z. Zhang, S.-M. Chen, Y.-Q. Yu, C.-Z. Lu. Chinese J. Struct. Chem. 21 (2002) 629.
- [22]H.H. Monfared, S. Alavi, R. Bikas, M. Vahedpour, P. Mayer. Polyhedron 29 (2010) 3355.

Table 1. Crystallographic and refinement data for the complexes

Complex	1	2	3
Formula	$C_{35}H_{36}Cl_4N_4O_{10}V_2$	$C_{18}H_{18}Cl_2FN_2O_5V$	$C_{19}H_{18}Cl_2F_3N_2O_5V$
Formula weight	916.36	483.18	533.19
Crystal shape/color	Block/brown	Block/brown	Block/brown
T (K)	298(2)	298(2)	298(2)
Crystal dimensions (mm ³)	$0.22 \times 0.20 \times 0.19$	$0.27 \times 0.27 \times 0.23$	$0.32 \times 0.27 \times 0.26$
Crystal system	Triclinic	Monoclinic	Triclinic
Space group	$P1$	Cc	$P-1$
a (Å)	7.556(2)	19.681(2)	7.991(2)
b (Å)	12.401(2)	15.091(2)	12.383(1)
c (Å)	12.462(2)	7.620(1)	13.232(1)
α (°)	70.346(2)	90	64.818(2)
β (°)	73.392(2)	109.147(2)	76.265(2)
γ (°)	76.727(2)	90	78.859(2)
V (Å ³)	1042.1(3)	2137.9(5)	1144.7(3)
Z	1	4	2
D_{calc} (g cm ⁻³)	1.460	1.501	1.547
μ (Mo K α) (mm ⁻¹)	0.762	0.754	0.724
$F(000)$	468	984	540
Measured reflections	5912	6234	6741
Unique reflections	4796	3516	4228
Observed	3232	2838	2948

reflections ($I \geq 2\sigma(I)$)			
Min. and max.	0.8503 and 0.8688	0.8224 and 0.8458	0.8014 and 0.8342
transmission			
Parameters	505	264	321
Restraints	6	2	68
Goodness of fit on F^2	1.073	1.034	1.109
$R_1, wR_2 [I \geq 2\sigma(I)]^a$	0.0675, 0.1534	0.0414, 0.0922	0.0765, 0.2009
R_1, wR_2 (all data) ^a	0.1079, 0.1923	0.0569, 0.1048	0.1082, 0.2214

$$^a R_1 = F_o - F_c/F_o, wR_2 = [\sum w(F_o^2 - F_c^2)/\sum w(F_o^2)^2]^{1/2}$$

Table 2. Selected bond distances (Å) for the complexes

1			
V1-O5	1.572(8)	V1-O4	1.747(7)
V1-O1	1.850(8)	V1-O2	1.930(7)
V1-N1	2.141(9)	V1-O3	2.391(8)
V2-O10	1.572(8)	V2-O9	1.766(7)
V2-O6	1.873(8)	V2-O7	1.919(7)
V2-N3	2.140(8)	V2-O8	2.374(7)
O5-V1-O4	103.0(4)	O5-V1-O1	99.4(4)
O4-V1-O1	100.6(4)	O5-V1-O2	98.8(4)
O4-V1-O2	95.8(3)	O1-V1-O2	152.0(3)
O5-V1-N1	94.3(4)	O4-V1-N1	161.3(3)
O1-V1-N1	83.5(3)	O2-V1-N1	74.0(3)
O5-V1-O3	174.8(3)	O4-V1-O3	82.2(3)
O1-V1-O3	80.0(4)	O2-V1-O3	79.9(3)
N1-V1-O3	80.5(3)	O10-V2-O9	103.8(4)
O10-V2-O6	99.9(4)	O9-V2-O6	101.1(3)
O10-V2-O7	98.7(4)	O9-V2-O7	94.3(3)
O6-V2-O7	152.2(3)	O10-V2-N3	94.4(3)
O9-V2-N3	159.8(3)	O6-V2-N3	84.2(3)
O7-V2-N3	73.9(3)	O10-V2-O8	174.6(3)
O9-V2-O8	81.6(3)	O6-V2-O8	79.4(3)
O7-V2-O8	80.1(3)	N3-V2-O8	80.2(3)
2			
V1-O5	1.555(3)	V1-O4	1.752(3)

V1-O1	1.861(3)	V1-O2	1.920(3)
V1-N1	2.143(3)	V1-O3	2.345(3)
O5-V1-O4	103.18(15)	O5-V1-O1	98.31(18)
O4-V1-O1	101.63(14)	O5-V1-O2	99.37(16)
O4-V1-O2	94.42(14)	O1-V1-O2	152.67(13)
O5-V1-N1	95.53(16)	O4-V1-N1	159.38(15)
O1-V1-N1	83.90(14)	O2-V1-N1	73.80(14)
O5-V1-O3	175.35(14)	O4-V1-O3	81.47(12)
O1-V1-O3	80.51(15)	O2-V1-O3	80.18(13)
N1-V1-O3	79.88(13)		
3			
V1-O5	1.572(4)	V1-O4	1.757(4)
V1-O1	1.858(4)	V1-O2	1.962(4)
V1-N1	2.138(4)	V1-O3	2.330(4)
O5-V1-O4	101.7(2)	O5-V1-O1	99.7(2)
O4-V1-O1	104.38(17)	O5-V1-O2	97.3(2)
O4-V1-O2	92.90(17)	O1-V1-O2	152.64(18)
O5-V1-N1	94.6(2)	O4-V1-N1	160.2(2)
O1-V1-N1	83.59(16)	O2-V1-N1	73.77(16)
O5-V1-O3	174.95(18)	O4-V1-O3	82.66(17)
O1-V1-O3	81.53(18)	O2-V1-O3	79.81(17)
N1-V1-O3	80.61(16)		

Table 3. Antimicrobial activities of the compounds with minimum inhibitory concentrations ($\mu\text{g}\cdot\text{mL}^{-1}$)

Tested material	<i>B. subtilis</i>	<i>S. aureus</i>	<i>E. coli</i>	<i>P. fluorescence</i>
H ₂ L ¹	75	37.5	> 150	> 150
H ₂ L ¹	18.8	37.5	75	> 150
H ₂ L ¹	9.4	18.8	18.8	> 150
1	18.8	18.8	37.5	> 150
2	2.3	1.2	18.8	> 150
3	1.2	2.3	9.4	> 150
Penicillin G	2.3	4.7	>150	> 150

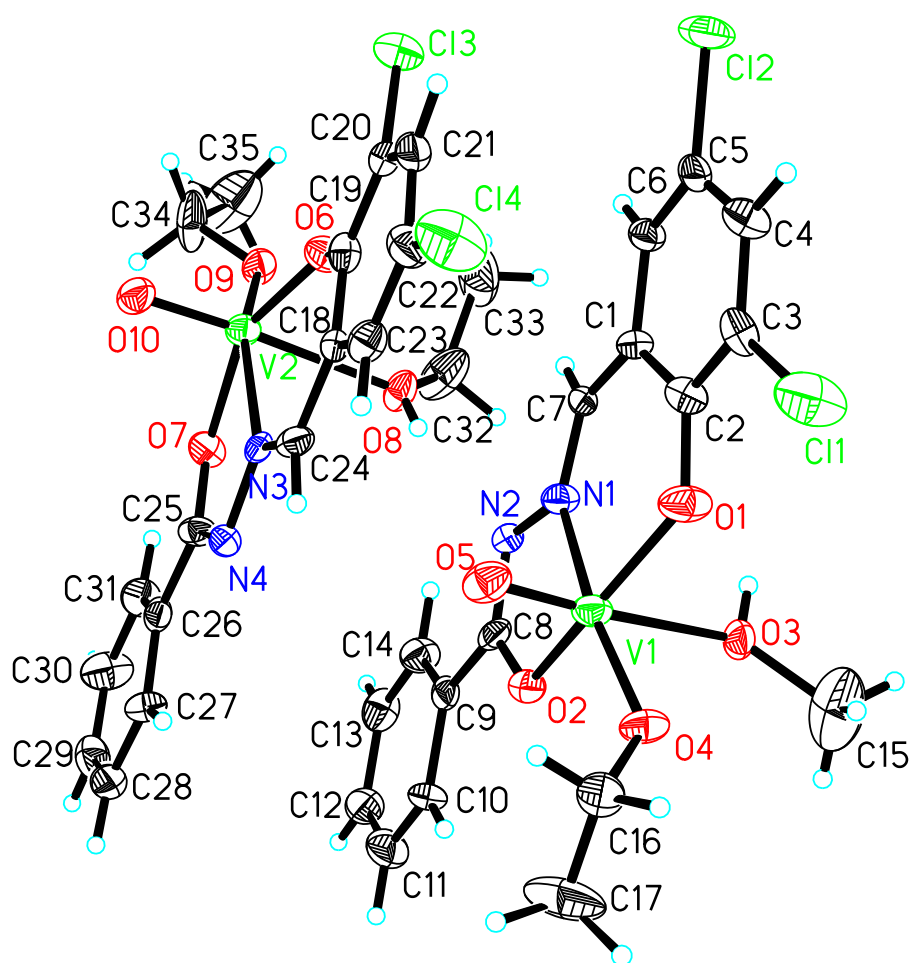


Figure 1. A perspective view of complex **1** with the atom labeling scheme. Thermal ellipsoids are drawn at the 30% probability level.

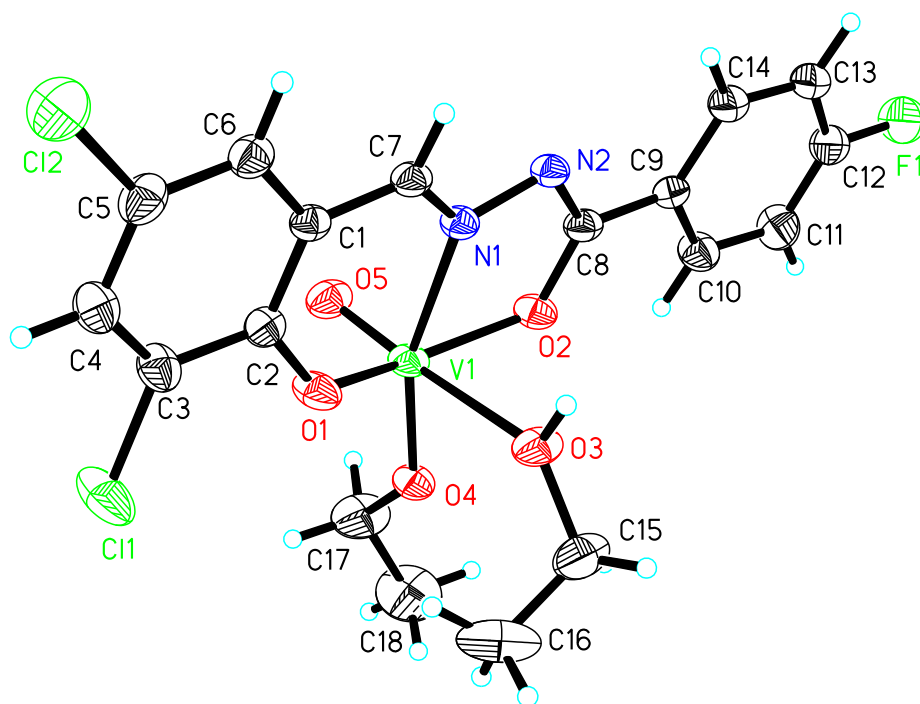


Figure 2. A perspective view of complex **2** with the atom labeling scheme. Thermal ellipsoids are drawn at the 30% probability level.

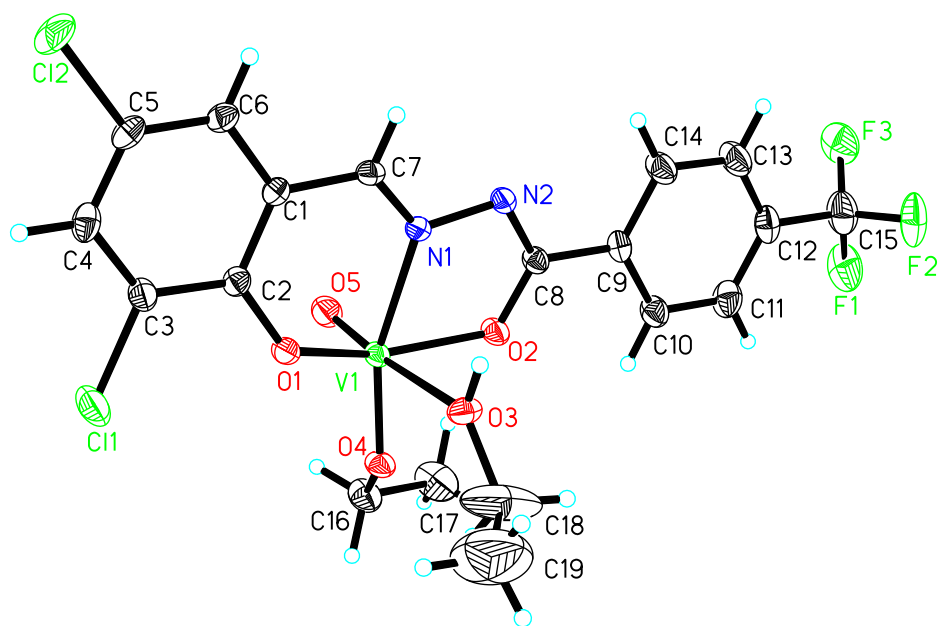


Figure 3. A perspective view of complex 3 with the atom labeling scheme. Thermal ellipsoids are drawn at the 30% probability level.

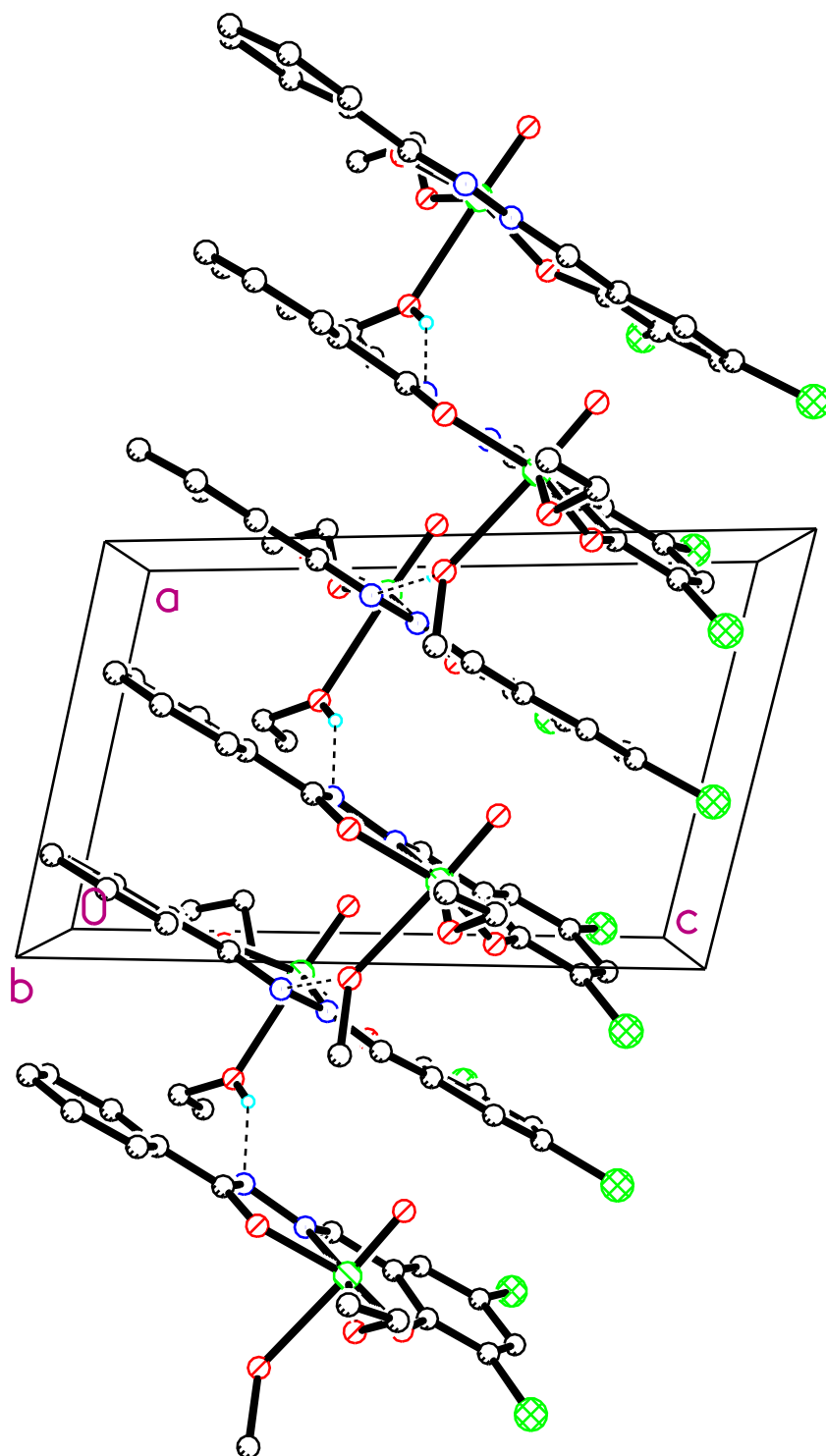


Figure 4. Molecular packing structure of complex **1**, with hydrogen bonds shown as dotted lines.

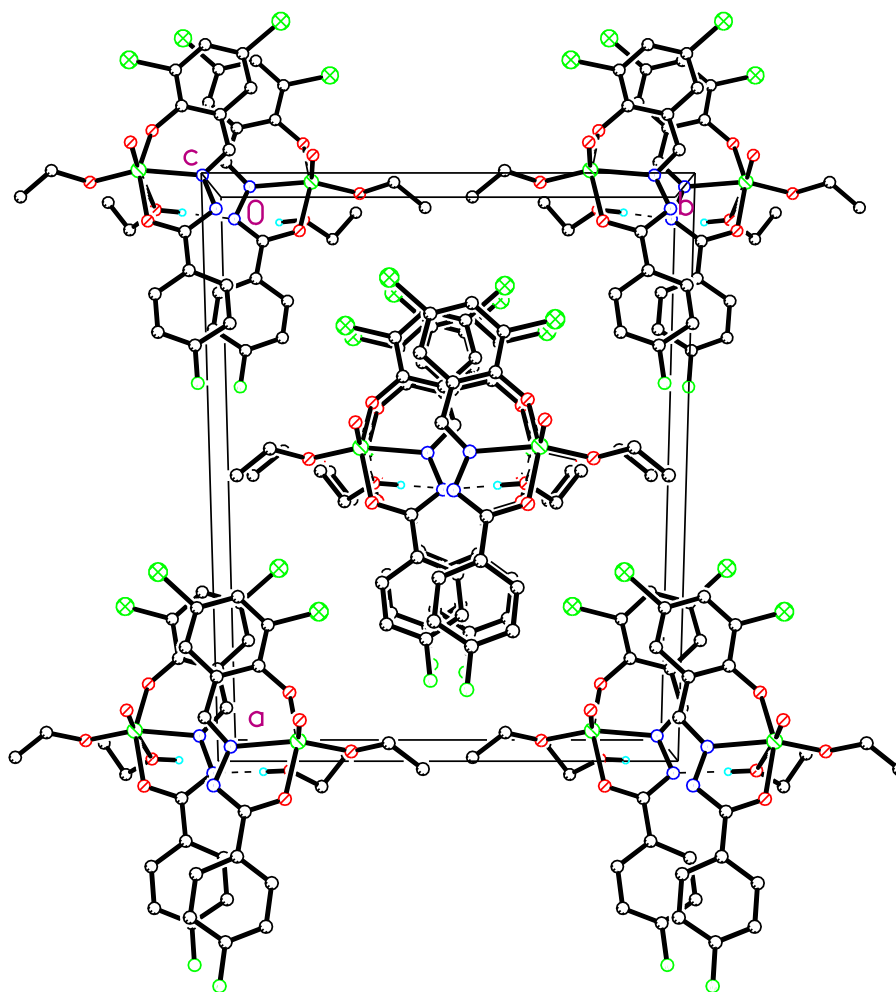


Figure 5. Molecular packing structure of complex **2**, with hydrogen bonds shown as dotted lines.

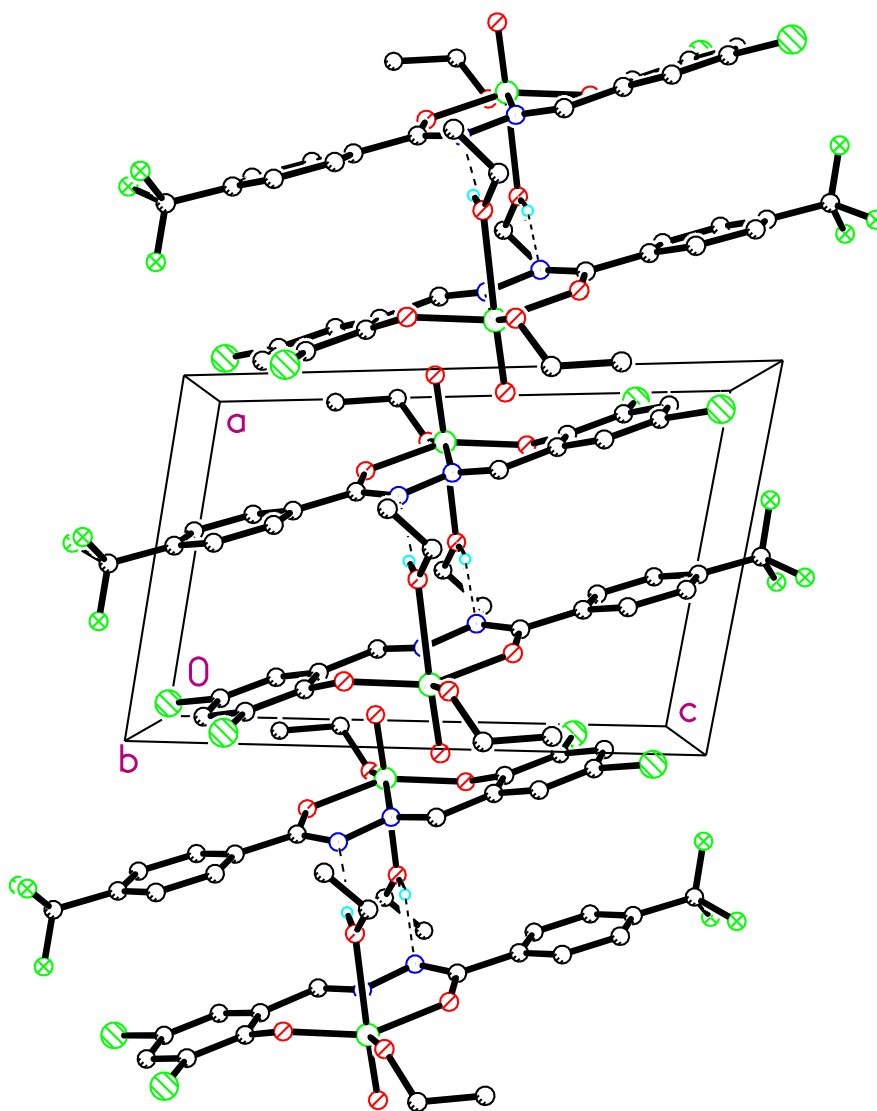
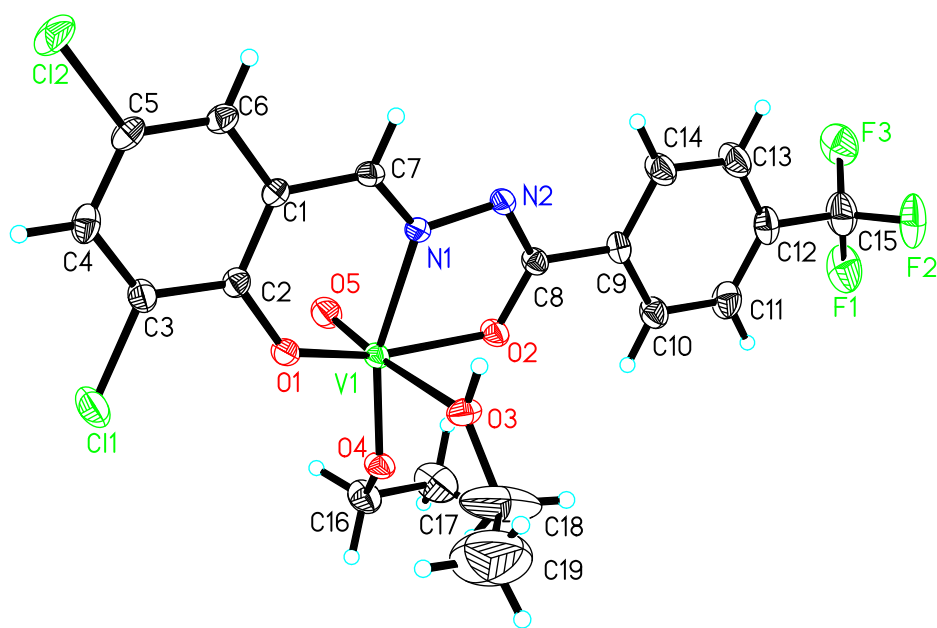


Figure 6. Molecular packing structure of complex **3**, with hydrogen bonds shown as dotted lines.



ACCEPTED MANUSCRIPT

Three new chlorido-substituted hydrazone compounds N' -(3,5-dichloro-2-hydroxybenzylidene)benzohydrazide (H_2L^1), N' -(3,5-dichloro-2-hydroxybenzylidene)-4-fluorobenzohydrazide (H_2L^2) and N' -(2-hydroxy-3-methylbenzylidene)-4-trifluoromethylbenzohydrazide (H_2L^3), were prepared and characterized. Based on the hydrazone compounds, three new vanadium(V) complexes, $[VOL^1(OEt)(EtOH)] \cdot [VOL^1(OEt)(MeOH)]$ (**1**), $[VOL^2(OEt)(EtOH)]$ (**2**) and $[VOL^3(OEt)(EtOH)]$ (**3**), were prepared and characterized. The hydrazone compounds and their vanadium complexes were evaluated on their antimicrobial activities. The existence of the fluoro groups in the hydrazone ligands can improve the activities.